Theoretical Study on the Reaction Mechanism of Vinyl Radical with Formaldehyde

Hong-bin Xie, Yi-hong Ding,* and Chia-chung Sun

State Key Laboratory of Theoretical and Computational Chemistry, Institute of Theoretical Chemistry, Jilin University, Changchun 130023, People's Republic of China

Received: May 7, 2005; In Final Form: July 11, 2005

A detailed computational study is performed on the radical−molecule reaction between the vinyl radical (C_2H_3) and formaldehyde (H_2CO), for which only the direct hydrogen abstraction channel has been considered by previous and very recent theoretical studies. At the Gaussian-3//B3LYP/6-31G(d) and CBS-QB3 levels, the direct H-abstraction forming C_2H_4 + HCO has barriers of 3.9 and 4.7 kcal/mol, respectively. The addition barrier to form H_2CCHCH_2O has barriers of 2.8 and 2.3 kcal/mol, respectively. Subsequently, there are two highly competitive dissociation pathways for H_2CCHCH_2O: One is the formation of the direct H-extrusion product $H_2CCHCHO$ + H, and the other is the formation of C_2H_4 + HCO via the intermediate H_2CCH_2-CHO. Surely, the released energy is large enough to drive the secondary dissociation of HCO to H + CO. Because the involved transition states and intermediates of the H_2CCHCH_2O evolution all lie energetically lower than the entrance addition transition state, the addition−elimination is more competitive than the direct H-transfer for the C_2H_3 + H_2CO reaction, in contrast to previous expectation. The present results can be useful for future experimental investigation on the title reaction.

1. Introduction

The vinyl radical (C_2H_3) is a reactive intermediate formed during oxidation of hydrocarbons and plays an important role in atmospheric and combustion chemistry.[1−14] It is of great significance to learn the behavior of the C_2H_3 radical for environmental protection. Up to now, a number of theoretical and experimental investigations have been performed on the C_2H_3 with atoms, radicals, and molecules such as O, NO, CH_3, H_2, C_2H_2, C_2H_4, CO, O_2, H_2CO, and so forth.[1−13]

As a prototypical aldehyde molecule, formaldehyde (H_2CO) is ubiquitous in the environment and is commonly found in air, water, and industrial products. Because of the importance and the simplicity, the H_2CO molecule has long been the subject of extensive spectroscopic,[15] photochemical,[16] and theoretical[17] investigations. Unfortunately, the compound is known to be mutagenic and carcinogenic. How to remove or prevent the formation of this pollutant molecule has become one of the most important environmental issues. Furthermore, H_2CO has been detected in space.[18] Knowledge of its reactions is important to understand its abundance, depletion mechanism, and potential role in synthesizing new interstellar molecules. Up to now, many radical−H_2CO reactions such as H, D, O(^{3}P), F, Cl, Br, CH_3, NH_2, OH, HO_2, BrO, CN, NO_3, and C_6H_5 have been studied by experimentalists and theoreticians.[19−35]

Both C_2H_3 and H_2CO may coexist during the photochemical oxidation or combustion of methane and other hydrocarbons and have also been found in space, so the reaction of C_2H_3 with H_2CO might influence the decay rate of the C_2H_3 radical and might further have an effect on the other chain reactions considered in combustion processes. Despite their importance in combustion and atmospheric chemistry, the reaction of the C_2H_3 radical with H_2CO has not been experimentally studied to the best of our knowledge. Theoretically, three groups including two early (from bond energy and bond order method)[7,11] and one very recent (from QCISD(T)/cc-pVTZ//MP2/cc-pVDZ)[13] have investigated the title reaction. Yet, they only considered the direct hydrogen-abstraction process and calculated the rate constants. This seems to be reasonable, because for most of the previously studied radical−H_2CO reactions, direct H-abstraction is more competitive than addition−elimination. However, we are aware that the addition−elimination process for the R + H_2CO reaction is actually very complex. The kinetics of both the entrance and further dissociation or isomerization processes of the addition isomer RCH_2O cooperatively determine the overall mechanism. Therefore, it is quite desirable to carry out a detailed mechanistic study on the experimentally unknown C_2H_3 + H_2CO reaction at a more reliable computational level than previously applied. Such a study is reported in the present paper. It will be shown that, contrary to the previous expectation of the direct H-abstraction process for the title reaction, the C_2H_3 + H_2CO reaction favors an addition−elimination mechanism.

2. Computational Methods

All calculations were performed with the *Gaussian 98* program package.[36] Geometries were initially optimized at the B3LYP/6-31G(d) level. Harmonic vibrational frequencies were calculated to check whether the obtained species is a minimum isomer (with all real frequencies) or a transition state (with one and only one imaginary frequency). For each transition state, the intrinsic reaction coordinate (IRC) calculations were performed to guarantee its correct connection to the designated isomers. Finally, to obtain more reliable energetics, the Gaussian-3 calculations using the B3LYP/6-31G(d)-optimized geometries and frequencies (denoted as G3B3) were carried out.[37,38] For the important transition states, the CBS-QB3[39,40] method is also used.

3. Results and Discussion

For the title C_2H_3 + H_2CO reaction, Figure 1 depicts the structures of the most important reactants, products, isomers,

* E-mail: yhdd@mail.jlu.edu.cn. Fax: +86-431-8498889.

10.1021/jp052375i CCC: $30.25
Published on Web 08/23/2005

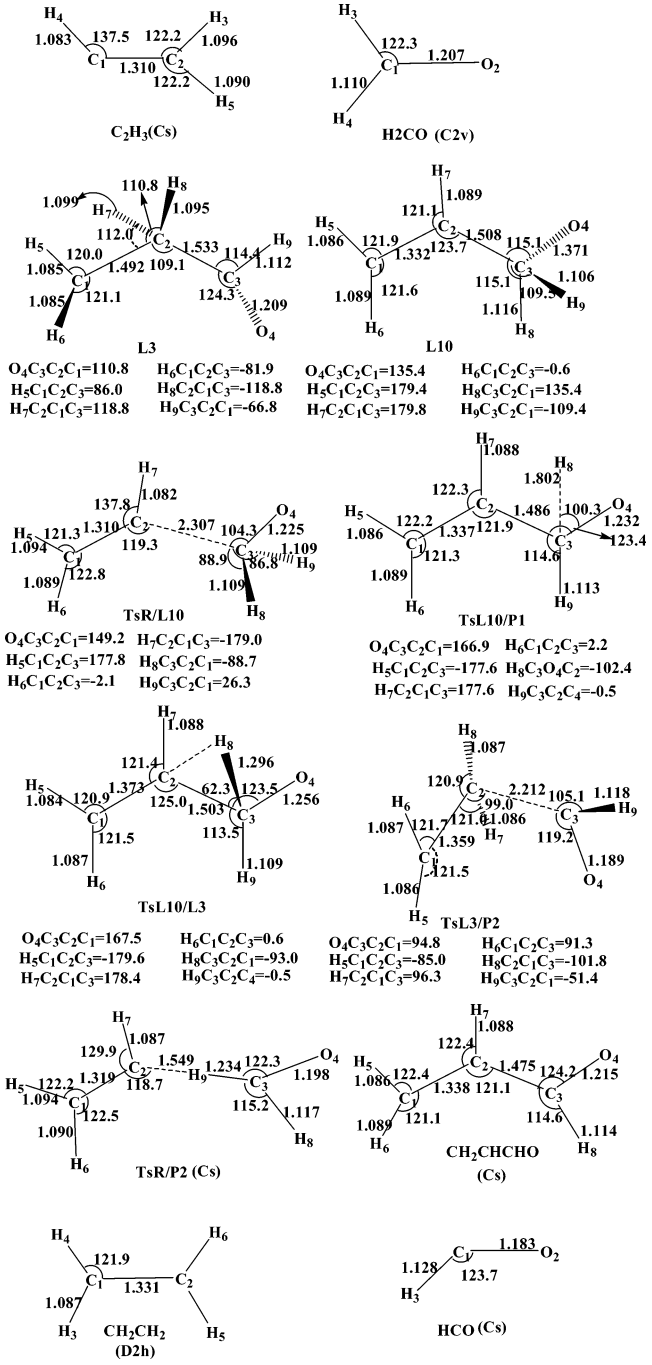

Figure 1. Optimized geometries of important isomers, interconversion transition states, and products for the $C_2H_3 + H_2CO$ reaction at the B3LYP/6-31G(d) level. Bond lengths are in angstroms and angles in degrees.

and transition states. The schematic potential energy surface (PES) of the $C_2H_3 + H_2CO$ reaction at the G3B3 level is presented in Figure 2a,b. The total energy of the reactant **R** $C_2H_3 + H_2CO$ is set as zero. The energetic data (G3B3) of the most important products, isomers, and transition states are listed in Table 1. The energetic information for the H-abstraction process including the reaction energies, the reaction enthalpies, and the forward and reverse classical potential barrier heights at the G3B3 and CBS-QB3 levels of theory are listed in Table 2 along with the available experimentally deduced thermochemical data[41] and very recent theoretical data.[13]

A. Entrance Channels. We first discuss the results based on the G3B3 PES. The attack of the C_2H_3 radical on the H_2CO molecule may have five possible entrance ways: (i) C-addition leading to H_2CCHCH_2O **L10** (−37.2); (ii) H-abstraction leading to **P2** $C_2H_4 + HCO$ (−21.6); (iii) O-addition leading to $H_2CCHOCH_2$ **L8** (−21.9); (iv) H-donation leading to **P7** $C_2H_2 + H_2COH$ (6.7); and (v) 2 + 2 cycloaddition leading to cCH_2CHOCH_2 **C8** (−17.7). The values in parentheses are relative energies in kilocalories per mole with reference to **R**. The corresponding barriers are 2.8 via **TsR/L10**, 4.7 via **TsR/P2**, 14.3 via **TsR/L8**, 33.5 via **TsR/P7**, and 70.7 kcal/mol via **TsR/C8**. Surely, the two former entrance channels are of most interest for combustion and atmospheric relevance. Particularly, the addition process forming **L10** is thermodynamically and kinetically more favorable than the direct H-abstraction, similar to the $CH_3 + H_2CO$ reaction.[42] We were unable to locate the transition states for the direct 1 + 2 cycloaddition forming $H_2C-cCOCH_2$ **C5** (−17.2) and direct 2 + 2 cycloaddition forming cCH_2CHCH_2O **C3** (−11.6). Here, the symbol **L** means chainlike structures, and the symbol **C** means cyclic structures.

B. Isomerization and Dissociation. Starting from the addition product H_2CCHCH_2O **L10**, which is the most favorable entrance channel, there are six possible reaction pathways: (i) ring closure leading to $H_2C-cCOCH_2$ **C5** (−17.2); (ii) H-extrusion leading to **P1** $H_2CCHCHO + H$ (−7.5); (iii) 1,2-H-shift forming H_2CCH_2CHO **L3** (−37.2); (iv) 1,2-H-shift forming $H_2CCHCHOH$ **L2** (−43.1); (v) 1,4-H-shift leading to $HCCHCH_2OH$ **L7** (−13.7); and (vi) ring closure leading to cCH_2CHCH_2O **C3** (−11.6). The corresponding transition states for the six channels are **TsL10/C5** (−11.9), **TsL10/P1** (−1.5), **TsL10/L3** (−0.9), **TsL10/L2** (4.1), **TsL10/L7** (5.3), and **TsL10/C3** (10.3). Because the latter three **TS**s lie higher in energy than the entrance **TsR/L10** (2.8), channels (iv)−(vi) can be excluded. Moreover, although formation of the three-membered ring isomer $H_2C-cCOCH_2$ **C5** in channel (i) has the lowest barrier, its further conversions are unfavorable, i.e., the chain isomer $H_2CCHOCH_2$ **L8** (−21.9) formed from **C5** via **TsC5/L8** (−4.5) would rather isomerize back to **C5** instead of rearranging to $HCCHOCH_3$ via **TsL8/L6** (8.9) or to cCH_2CHOCH_2 **C8** (17.7) via **TsL8/C8** (15.79). Therefore, channel (i) is expected to have little contribution to the final fragmentation.

The remaining two channels (ii) and (iii) (1,2-H-shift) have close barriers via **TsL10/P1** (−1.54) and **TsL10/L3** (−0.9). Channel (ii) is very simple and is associated with the direct H-extrusion forming propenal $H_2CCHCHO$, which has been recently identified in interstellar space.[43] However, channel (iii) is very complicated, as shown in Figure 2b. The low-lying intermediate H_2CCH_2CHO **L3** formed in channel (iii) has various evolution possibilities. We first can exclude the processes **L3** → O−$cCHCH_2CH_2$ **C4**, **L3** → cCH_2CHOCH_2 **C8**, **L3** → $CH_2CHCHOH$ **L2**, and **L3** → CH_2CH_2COH **L0**, because the first one has almost zero reverse barrier and the latter three have higher-energy transition states above that of the reactant **R**. The following processes including fragmentation could be of interest. Their pathways are schematically written as follows:

(a) **L3** → **P2** $C_2H_4 + HCO$.

(b) **L3** → CH_3CHCHO **L5** → **P1** $H_2CCHCHO + H$.

(c) **L3** → CH_3CHCHO **L5** → CH_3CH_2CO **L1** → **P3** $CH_2-CH_3 + CO$.

(d) **L3** → **P1** $H_2CCHCHO + H$.

(e) **L3** → CH_3CH_2CO **L1** → P3 $CH_2CH_3 + CO$.

The direct C−C rupture **TSL3/P2** (−14.2) of **L3** in path (a) is energetically much lower than the rate-determining transition

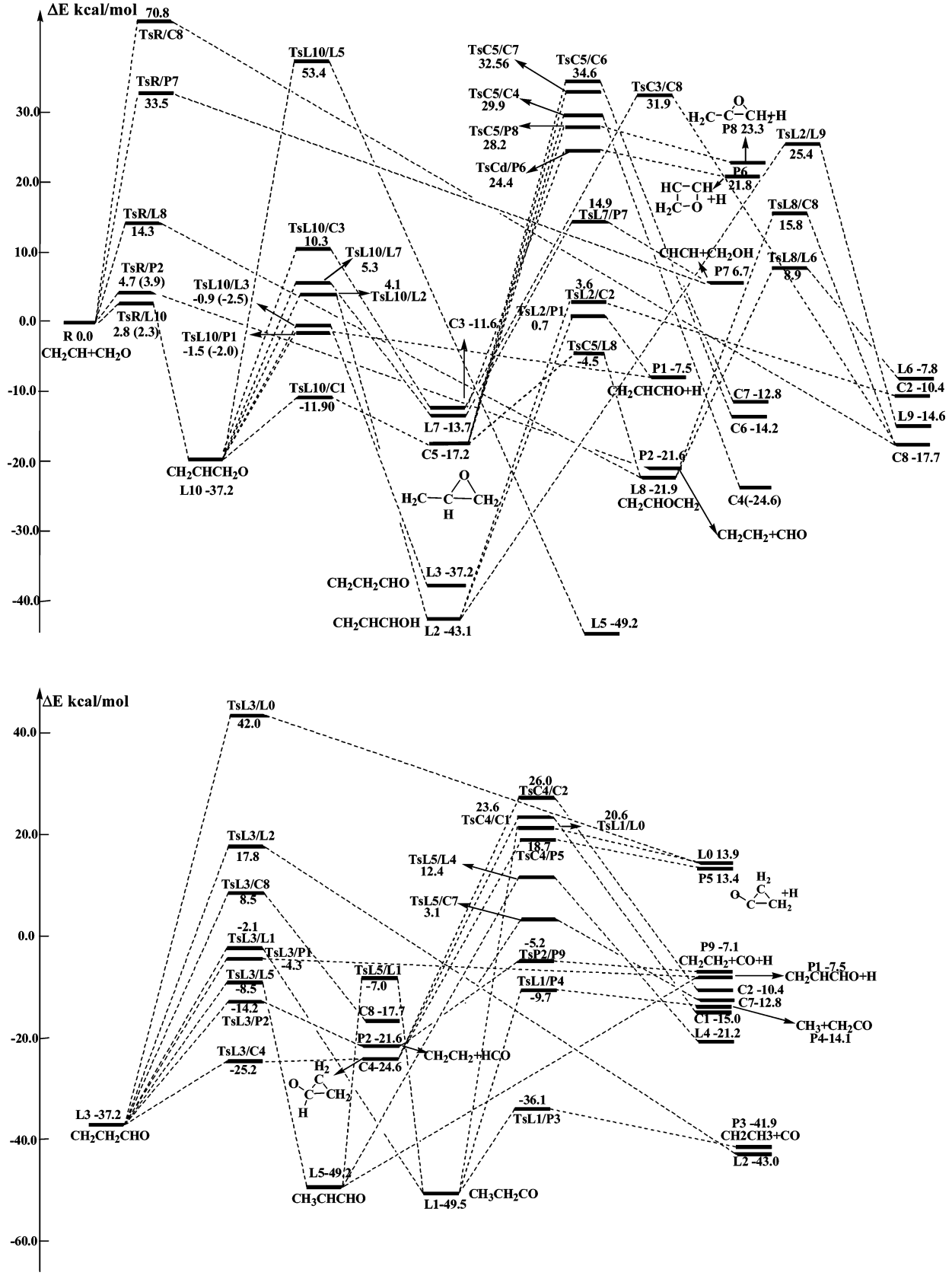

Figure 2. (a) Schematic potential energy surface of the $C_2H + H_2CO$ reaction at the Gaussian-3//B3LYP/6-31G(d) level showing various entrance channels and some conversion pathways starting from isomer CH_2CHCH_2O **L10**. The CBS-QB3 relative energies for some structures are also given in parentheses. (b) Schematic potential energy surface of the $C_2H_3 + H_2CO$ reaction at the Gaussian-3//B3LYP/6-31G(d) level showing the relevant conversion pathways of isomer CH_2CH_2CHO **L3**.

state in paths (b), (c), (d) and (e) by 6.7, 7.2, 9.9 and 12.1 kcal/mol, respectively. Surely, the most competitive pathway is the formation of **P2** $C_2H_4 + HCO$. This process is also very simple.

C. Reaction Mechanism and Implications. In summary, the former relevant pathways for the $C_2H_3 + H_2CO$ reaction at the G3B3 level can be written as follows.

TABLE 1: Total (au) and Relative (kcal/mol, in parentheses) Energies of the Reactant, Important Products, Intermediate Isomers, and Transition States at the G3B3 Level

species	G3B3	species	G3B3
R $C_2H_3 + H_2CO$	−192.26895 (0.)	TsR/P2	−192.26153 (4.7)
	−192.08712 (0.0)[a]		*−192.08097 (3.9)*
L3 CH_2CH_2CHO	−192.32824 (−37.2)	TsR/L10	−192.26447 (2.8)
			−192.08345 (2.3)
L10 CH_2CHCH_2O	−192.30060 (−37.2)	TsL10/L3	−192.27037 (−0.9)
			−192.09104 (−2.5)
P2 $CH_2CH_2 + CHO$	−192.30339 (−21.6)	TsL10/P1	−192.27136 (−1.5)
			−192.09037 (−2.0)
P1 $CH_2CHCHO + H$	−192.28085 (−7.5)	P9 $CH_2CH_2 + H + CO$	−192.28026 (−7.1)

[a] The italic values are at the CBS-QB3 level.

TABLE 2: The Reaction Energetics Parameters (kcal/mol) for the H-Abstraction at the Various Levels of Theory

method	ΔE[a]	$\Delta H_{298.15K}$	$V_f^{\neq}$[b]	$V_f^{\neq}$[c]
G3B3	−21.6	−21.7	4.7	26.3
CBS-QB3	−21.5	−21.5	3.9	25.3
PMP4/cc-pVTZ//MP2/cc-pVDZ[d]	−24.6	−25.0	5.3	30.8
QCISD(T)/cc-pVTZ//MP2/cc-pVDZ[d]	−23.3	−23.8	5.8	30.1
exptl[e]		-22.5 ± 2		

[a] Reaction energy. [b] Forward classical barrier height. [c] Reverse classical barrier height. [d] Ref 13. [e] Ref 41.

Path 1i: **R** $C_2H_3 + H_2CO \rightarrow H_2CCHCH_2O$ **L10** → **P1** $H_2CCHCHO + H$.

Path 1ii: **R** $C_2H_3 + H_2CO \rightarrow H_2CCHCH_2O$ **L10** → H_2CCH_2CHO **L3** → **P2** $C_2H_4 + HCO$ → **P9** $C_2H_4 + CO + H$.

Path 2: **R** $C_2H_3 + H_2CO$ → **P2** $C_2H_4 + HCO$ → **P9** $C_2H_4 + CO + H$.

Path 1i and **Path 1ii** belong to the addition−elimination mechanism, whereas **Path 2** belongs to the direct H-abstraction mechanism. In **Path 1i** and **Path 1ii**, the entrance channel is the rate-determining step. Note that the **P2** $C_2H_4 + HCO$ → **P9** $C_2H_4 + CO + H$ process is associated with the secondary dissociation, because the latent energy of **P2**, −21.6 kcal/mol, is large enough to overcome the direct C−H rupture barrier (16.4 kcal/mol) of HCO.

Additionally, at the CBS-QB3 level, the transition states **TsR/L10**, **TsR/P2**, **Tsa/P1**, and **TsL10/L3** have the respective relative energies 2.3, 4.7, −2.5, and −2.0 kcal/mol with respect to **R**. The corresponding G3B3 relative energies are 2.8, 3.9, −1.5, and −0. 9 kcal/mol. Surely, both high-level calculations definitively predict that the addition−elimination process is more competitive than the direct H-abstraction one.

To guarantee the reliability of the theory used here, it is worthwhile to compare our results with the available experimentally deduced thermochemical data[41] and very recent theoretical data[13] for the H-abstraction process. As can be seen from Table 2, the predicted reaction enthalpies of −21.7 and −21.5 kcal/mol for this process at the G3B3 and CBS-QB3 levels, respectively, are closer to the experimental value of -22.5 ± 2 than the very recent theoretical values of −23.8 and −25.0 kcal/mol at the QCISD(T)/cc-pVTZ//MP2/cc-pVDZ and PMP4/cc-pVTZ//MP2/cc-pVDZ levels, respectively. Thus, the present more composite G3B3 and CBS-QBS methods are expected to provide more reliable results than those previously applied. Moreover, both the G3B3 and CBS-QB3 methods predict much lower H-abstraction barriers (4.7 and 3.9 kcal/mol, respectively) than the QCISD(T)/cc-pVTZ//MP2/cc-pVDZ and PMP4/cc-pVTZ//MP2/cc-pVDZ values (5.8 and 5.3 kcal/mol, respectively). The direct H-abstraction process is faster than previously expected.

Although a large number of radical−H_2CO reactions have been extensively studied,[19−35] the $C_2H_3 + H_2CO$ reaction has never been investigated experimentally. This reaction could play an important role in the burning or oxidation of hydrocarbons. The three available theoretical studies have only considered the direct H-abstraction mechanism. The present detailed mechanistic study may thus provide useful information for future experiments. However, the existence of sizable barriers suggests that the $C_2H_3 + H_2CO$ reaction may be less likely in interstellar regions where the temperature is usually very low.

4. Conclusions

In contrast to the previous theoretical studies, the present Gaussian-3//B3LYP/6-31G(d) and CBS-QB3 computational methods both predict that the addition−elimination process is more competitive than direct H-abstraction. The entrance addition barriers are 2.8 and 2.3 kcal/mol, respectively, at the two levels leading to H_2CCHCH_2O, which can competitively generate $H_2CCHCHO + H$ and $C_2H_4 + HCO$. The direct H-abstraction barriers are 3.9 and 4.7 kcal/mol, respectively. The secondary dissociation of HCO to H + CO is possible with the released energy. The present results can provide useful information for future experimental investigation on the title reaction.

Acknowledgment. This work was supported by the National Natural Science Foundation of China (20103003), Excellent Young Teacher Foundation of Ministry of Education of China.

Supporting Information Available: For all the fragments, isomers, and transition states, the structural parameters are listed in SIFigure 1 and the total and relative energies are listed in SITable 1. This material is available free of charge via the Internet at http://pubs.acs.org.

References and Notes

(1) Fahr, A.; Monks, P. S.; Stief, L. J.; Laufer, A. H. **1995**, *116*, 415.
(2) Knyazev, V. D.; Bencsura, A.; Stoliarov, S. I.; Slagle, I. R. *J. Phys. Chem.* **1996**, *100*, 11346.
(3) Duran, R. P.; Amorebieta, V. T.; Colussi, A. J. *Int. J. Chem. Kinet.* **1989**, *21*, 947.
(4) Weissman, M.; Benson, S. W. *Int. J. Chem. Kinet.* **1984**, *16*, 307.
(5) Thorn, R. P.; Payne, W. A.; Chillier, X. D. F.; Stief, L. J.; Nesbitt, F. L.; Tardy, D. D. *Int. J. Chem. Kinet.* **2000**, *32*, 304.
(6) Fahr, A.; Laufer, A. H.; Tardy, D. C. *J. Phys. Chem. A* **1999**, *103*, 8433.
(7) Tsang, W.; Hampson, R. F. *J. Phys. Chem. Ref. Data* **1986**, *15*, 1087.
(8) Mebel, A. M.; Diau, E. W. G.; Lin, M. C.; Morokuma, K. *J. Am. Chem. Soc.* **1996**, *118*, 9759.
(9) Benson, S. W. *Int. J. Chem. Kinet.* **1994**, *26*, 997.
(10) Heinemann, P.; Hofmann-Sievert, R.; Hoyermann, K. *Symp. Int. Combust. Proc.* **1998**, *21*, 865.
(11) Scherzer, K.; Loser, U.; Stiller, W. *Z. Chem.* **1987**, *27*, 300.
(12) Garrett, B. C.; Truhlar, D. G. *J. Chem. Phys.* **1979**, *70*, 1593.
(13) Zhang, Y.; Zhang, S. W.; Li Q. S. *Chem. Phys.* **2004**, *306*, 51−56.
(14) Laufer, A. H.; Fahr, A. *Chem. Rev.* **2004**, *104*, 2813.

(15) For example, see Terentis, A. C.; Kable, S. H. *Chem. Phys. Lett.* **1996**, *258*, 626.
(16) For example, see Smith, G. D.; Molina, L. T.; Molina, M. J. *J. Phys. Chem. A* **2002**, *106*, 1233.
(17) For example, see Zhang, X.; Zou, S.; Harding, L. B.; Bowman, J. M. *J. Phys. Chem. A* **2004**, *108*, 8980.
(18) Barbe, A.; Marche, P.; Secroun, C.; Jouve, P. *Geophys. Res. Lett.* **1979**, *6*, 463.
(19) Oehlers, C.; Wagner, H. Gg.; Ziemer, H.; Temps, F.; Dobe, S. *J. Phys. Chem. A* **2000**, *104*, 10500.
(20) Chang, J. S.; Barker, J. R. *J. Phys. Chem.* **1979**, *83*, 3059.
(21) Ferrieri, R. A.; Wolf, A. P. *J. Phys. Chem.* **1992**, *96*, 7164.
(22) Beukes, J.; D'Anna, A.; Bakken, B. V.; Nielsen, C. J. *Phys. Chem. Chem. Phys.* **2000**, *2*, 4049.
(23) Feilberg, K. L.; Johnson, M. S.; Nielsen, C. J. *J. Phys. Chem. A* **2004**, *108*, 7393.
(24) Liu, J. Y.; Li, Z. S.; Wu, J. Y.; Wei, Z. G.; Zhang, G.; Sun, C. C. *J. Chem. Phys.* **2003**, *119*, 7214, and references therein.
(25) Li, Q. S.; Lu, R. H. *J. Phys. Chem. A* **2002**, *106*, 9446.
(26) Butkovskaya, N. I.; Setser, D. W. *J. Phys. Chem. A* **1998**, *102*, 9715.
(27) Alvarez-Idaboy, J. R.; Mora-Diez, N. R.; Boyd, J.; Vivier-Bunge, A. *J. Am. Chem. Soc.* **2001**, *123*, 2018.
(28) D'Anna, B.; Bakken, V.; Beukes, J. A.; Nielsen, C. J.; Brudnik, K.; Jodkowski, J. T. *Phys. Chem. Chem. Phys.* **2003**, *5*, 1790.
(29) Barnes, I.; Becker, K. H.; Fink, E. H.; Reimer, A.; Zabel, F.; Niki, H. *Chem. Phys. Lett.* **1985**, *115*, 1.
(30) Jemi-Alade, A. A.; Lightfoot, P. D.; Lesclaux, R. *Chem. Phys. Lett.* **1992**, *195*, 25.
(31) Pinceloup, S.; Laverdet, G.; Maguin, F.; Doussin, J. F.; Carlier, P.; Bras, G. L. *J. Photochem. Photobiol., A* **2003**, *157*, 275.
(32) Hansen, J. C.; Li, J Y.; Francisco, S.; Li, Z. *J. Phys. Chem. A* **1999**, *103*, 8543.
(33) Feng, W. L.; Wang, Y. S.; Zhang, W.; Pang, X. Y. *Chem. Phys. Lett.* **1997**, *266*, 43.
(34) Choi, Y. M.; Xia, W. S.; Park, J.; Lin, M. C. *J. Phys. Chem. A* **2000**, *104*, 7030.
(35) Xia, W. S.; Lin, M. C. *Phys. Chem. Chem. Phys.* **2000**, *2*, 5566.
(36) Frisch, M. J.; Trucks, G. W.; Schlegel, H. B.; Scuseria, G. E.; Robb, M. A.; Cheeseman, J. R.; Zakrzewski, V. G.; Montgomery, J. A., Jr.; Stratmann, R. E.; Burant, J. C.; Dapprich, S.; Millam, J. M.; Daniels, A. D.; Kudin, K. N.; Strain, M. C.; Farkas, O.; Tomasi, J.; Barone, V.; Cossi, M.; Cammi, R.; Mennucci, B.; Pomelli, C.; Adamo, C.; Clifford, S.; Ochterski, J.; Petersson, G. A.; Ayala, P. Y.; Cui, Q.; Morokuma, K.; Malick, D. K.; Rabuck, A. D.; Raghavachari, K.; Foresman, J. B.; Cioslowski, J.; Ortiz, J. V.; Stefanov, B. B.; Liu, G.; Liashenko, A.; Piskorz, P.; Komaromi, I.; Gomperts, R.; Martin, R. L.; Fox, D. J.; Keith, T.; Al-Laham, M. A.; Peng, C. Y.; Nanayakkara, A.; Gonzalez, C.; Challacombe, M.; Gill, P. M. W.; Johnson, B. G.; Chen, W.; Wong, M. W.; Andres, J. L.; Head-Gordon, M.; Replogle, E. S.; Pople, J. A. *Gaussian 98*, revision A.11; Gaussian, Inc.: Pittsburgh, PA, 1998.
(37) Curtiss, L. A.; Raghavachari, K.; Redfern, P. C.; Rassolov, V.; Pople, J. A. *J. Chem Phys.* **1998**, *109*, 7764.
(38) Boboul, A. G.; Curtiss, L. A.; Redfern, P. C.; Raghavachari, K. *J. Chem. Phys.* **1999**, *110*, 7650.
(39) Montgomery, J. A., Jr.; Frisch, M. J.; Ochterski, J. W.; Petersson, G. A. *J. Chem. Phys.* **2000**, *112*, 6532.
(40) Montgomery, J. A., Jr.; Frisch, M. J.; Ochterski, J. W.; Petersson, G. A. *J. Chem. Phys.* **1999**, *110*, 2822.
(41) Chase, M. W., Jr. NIST-JANAF Themochemical Tables; *J. Phys. Chem. Ref. Data* **1998**; Monograph 9.
(42) Liu, J. Y.; Li, Z. S.; Wu, J. Y.; Wei, Z. G.; Zhang, G.; Sun, C. C. *J. Chem. Phys.* **2003**, *119*, 7214.
(43) Jewell, J. M.; Lovas, P. R.; Remjian, F. J. A.; Møllendal, H. *Ap. J. Letters* **2004**, *610*, L21.